# Printed Temperature Sensor Based on PEDOT: PSS-Graphene Oxide Composite

Mahesh Soni, *Member, IEEE*, Mitradip Bhattacharjee, *Member, IEEE*, Markellos Ntagios, and Ravinder Dahiya , *Fellow, IEEE*

Abstract—Temperature sensing is an important parameter needed to be measured by the eSkin during the physical interaction of robots with real-world objects. Yet, most of the work on sensors in eSkin has focused on pressure sensing. Here we present a skin conformable printed temperature sensor with poly(3,4-ethylenedioxythiophene): poly (styr-enesulfonate) (PEDOT:PSS)-graphene oxide (GO) as a temperature sensitive layer and silver (Ag) as contact electrodes. The demonstration of PEDOT:PSS/GO as a highly temperature sensitive layer is the distinct feature of the work. The response of presented sensor observed over ~25 °C (room temperature (RT)) to 100°C, by measuring the variation in resistance across the GO/PEDOT:PSS layer showed ~80% decrease in resistance. The sensitivity of the sensor was found to be 1.09% per °C. The sensor's response was also observed under static and dynamic bending (for 1000 cycles) conditions. The stable and repeatable response of sensor, in both cases, signifies strong adhesion of the layers with negligible delamination or debonding. In comparison to the commercial thermistor, the printed GO/PEDOT:PSS sensor is faster (~73% superior) with response and recovery times of 18 s and 32 s respectively. Finally, the sensor was attached to a robotic hand to allow the robot to act by using temperature feedback.

Index Terms—Temperature sensor, eSkin, printed electronics, tactile skin, robotics.
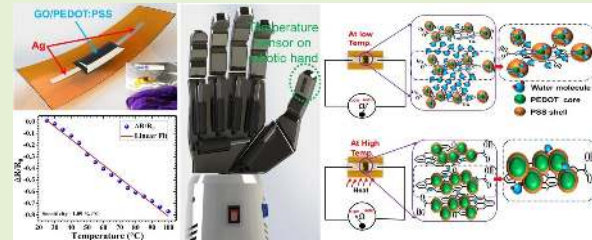
Response of printed flexible temperature sensor integrated on a robotic hand and the microstrucutral changes in the sensitive layer with temperature variations

I. INTRODUCTION

ELECTRONIC skin (eSkin) for robotics has attracted significant interest in recent years as it is critical for safe manipulation and exploration of objects and for safe human-machine interaction. The increasing focus on haptic feedback in new applications such as autonomous vehicles and in industry 4.0 settings are also contributing to the advances in eSkin technology. The contact force or pressure and the temperature are the most important parameters needed in these applications. Yet, most of the work on sensors in the eSkin has focused on pressure or force sensing as evident from wide variety of pressure/force and strain sensors developed using various organic/inorganic materials [1]–[4]. The accurate mea-surement of the variations in the skin temperature is needed for applications ranging from health monitoring to robotics [5]. In humans, the variations in skin temperature can be used for investigation of physical activities, cardiovascular health, and several other health diagnostics methods [6]–[10]. Likewise, the measurement of the variations in temperature is needed to mimic the functionalities of human skin in robotics and prosthetic applications [11], [12]. For example, an integrated temperature sensor can help the robots to distinguish between the hot and cold objects [12]–[14].

A wide variety of temperature sensors have been reported in the past using materials such as semiconductors, metals, metal oxides, and ceramics, etc. [15]–[19]. The resistive tem-perature sensors are most widely reported owing to their rapid response, stability, and accuracy [9], [20]. A few eSkins have also included temperature sensors that are based on silicon diodes or transistors [18], [21] developed using standard microfabrication techniques and the devices are not necessary flexible [22]–[24]. Most of the time, the complex processing and higher temperatures needed in standard microfabrication are not suitable with flexible substrates [1]–[4], [22]–[26]. In this regard, printed technologies offer an attractive alternative route for devices [11], [12], [27]–[30]. The interest in printed electronics is mainly because of the advantages such as substantial reduction in cost of fabrication, ease of printing on flexible substrates over large areas, integration of electronics directly on objects, etc. [1]–[4], [12], [28], [31].
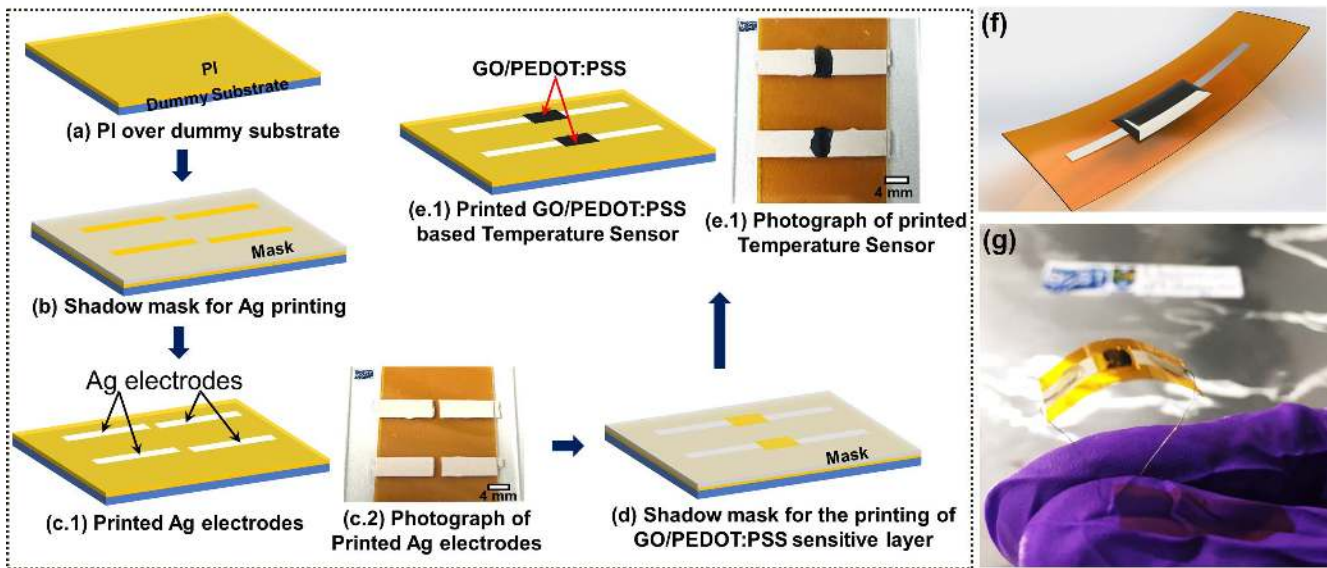
Fig. 1. (a) – (e) The process flow for fabrication of printed GO/PEDOT:PSS based temperature sensor; (f) Schematic image of fabricated temperature sensor; (g) Optical photograph for printed flexible temperature sensor.

These advantages of printed technologies have been exploited to develop various physical sensors (e.g. temperature [32], strain [12], [33]–[35], humidity, radio frequency identification (RFID) tags [36]) capable to detect and acquire data in real-time.

Typically, the printed resistive temperature sensors make use of conductive organic polymers as the temperature-sensitive layer [37]. The most widely used temperature sensitive layer include poly(3,4-ethylenedioxythiophene): poly (styr-enesulfonate) (PEDOT:PSS) [38], carbon nanotubes (CNTs) [39], PEDOT:PSS/CNT composite [37], [40], graphene oxide (GO) [7], [41], silver (Ag) [42], gold/chrome (Au/Cr) [43]. They offer excellent electrical conductivity and optical transparency [37]. Apart from these properties the thermal activation of PEDOT:PSS, GO promotes their use for temperature-sensitive layer [44]. However, the temperature sensors developed using these materials offer limited sensitivity ($< 0.6\%$ per °C) and the slow response and recovery times.

Herein we present highly sensitive ($>1\%$ per °C) printed temperature sensors on flexible polyimide (PI) substrates by using a simple, cost-effective and one-step fabrication route. We have utilized conductive silver (Ag) paste as the contact electrodes, while the PEDOT:PSS functionalized with GO (GO/PEDOT:PSS) composite was utilized as the temperature-sensitive layer. Owing to excellent adhesion and electrical performances with the flexible PI, the Ag paste is a good conductive material for the presented sensor [2], [4]. The biocompatibility, insulating nature and the presence of functional groups in GO allow strong functionalization of conducting and temperature-dependent PEDOT:PSS [44], [45]. The performance of printed temperature sensors was evaluated over temperatures ranging from room temperature (RT) to 100 °C. The work presented in this paper extends our previous work presented at IEEE FLEPS 2019 conference [32]. With respect to the preliminary work presented in the conference, herein we have further discussed the sensing in detail and analysed the sensors for the effect of bending. In addition, the printed sensor was attached to the thumb of robotic hand with feedback to identify hot objects.

This paper is organised as follows: Section II presents the fabrication and characterisation of the sensor. The results related to the presented temperature sensor are described in Section III. Finally, the key outcomes are summarised in Section IV.

II. FABRICATION AND CHARACTERISATION

A. Materials

The Ag conductive ink (186-3600) and PEDOT:PSS were purchased from RS components and Sigma Aldrich, UK respectively.

B. Fabrication

The fabrication steps for printed GO/PEDOT:PSS temperature sensor are illustrated in Fig.1. The commercially available PI substrates (thickness ~ 60 μm) was cut into 3 cm $\times$ 5 cm (L $\times$ W). The Ag conductive ink was printed on the PI substrates with the help of a shadow mask (Fig. 1(b)) followed by drying at 80 °C for 30 min (Fig. 1(c)). After drying, the dimension of each Ag electrodes was 1.3 cm in length and 4 mm in width, with the separation of 2 mm. The GO powder was synthesized using the modified Hummers method, as described in [45], [46]. The 1 mg/ml GO powder was dispersed in DI water under mild sonication. Finally the GO dispersion and PEDOT:PSS in the ratio 1:1 were mixed under constant stirring at 1000 rpm for 30 minutes. After this ~ 20 μl of the GO/PEDOT:PSS ink was drop casted over the Ag/PI as shown in Fig. 1(d) and Fig. 1(e). The optical image and the photograph of printed flexible GO/PEDOT:PSS based temperature sensor is shown in Fig. 1(f) and Fig. 1 (g), respectively. The sensitive layer of the printed flexible devices was insulated with Kapton tape (thickness ~ 50 μm) to minimize the effect of humidity and other environmental factors.
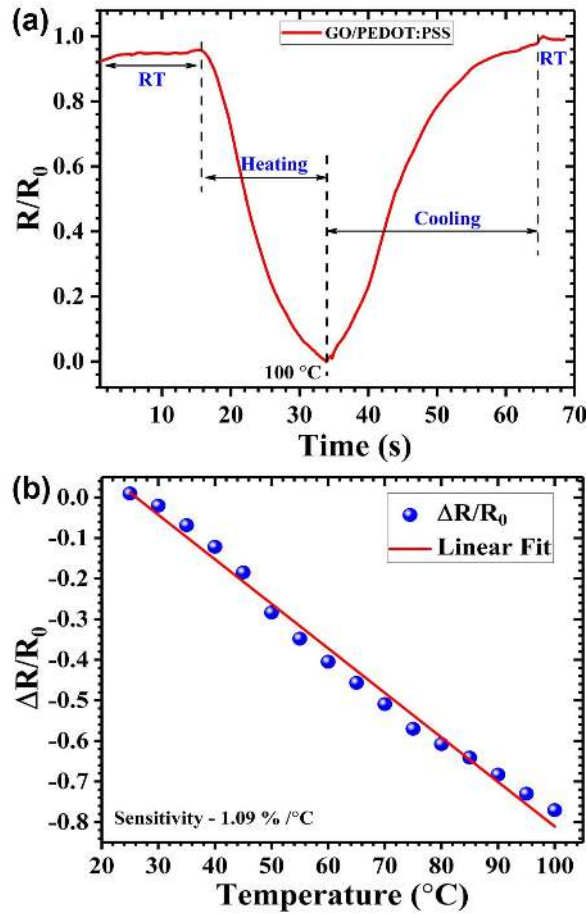
Fig. 2. (a) Relative change in resistance of the printed GO/PEDOT:PSS based temperature sensor over time from RT to 100 °C and back to RT. (b) The response ($\Delta R/R_0$) of the sensor as a function of temperature varying from RT to 100 °C.

C. Characterization

The change in the resistance of the printed flexible sensor as a function of temperature was measured using a LabView controlled Agilent 34461A series multimeter. The temperature of the hot plate was calibrated using a high precision IR thermometer (FLUKE 62 MAX). The bending measurements were carried out using the inhouse build setup reported elsewhere [47]. The robotic hand used in the study was 3D printed in the lab [12].

III. RESULTS AND DISCUSSIONS

The normalized resistance (R/R_0, where R is the sensor resistance and R_0 is the base resistance at RT) of the printed GO/PEDOT:PSS based temperature sensor over time, as shown in Fig. 2(a). Initially the sensor was placed over a hot plate maintained at room temperature (RT) to get the stable response of the sensor. A minimal variation of ∼ 2% in R/R₀ at RT with respect to the response of the sensor can be observed in Fig. 2 (a) for initial 15 s. This variation may be attributed to the minute self-adjustment of polymer-GO composite in the polymer matrix due to thermal coefficients and local change in the effective relative humidity, as reported in [48]. However, to minimize the effect of humidity and other environmental factors, the sensitive layer of the printed
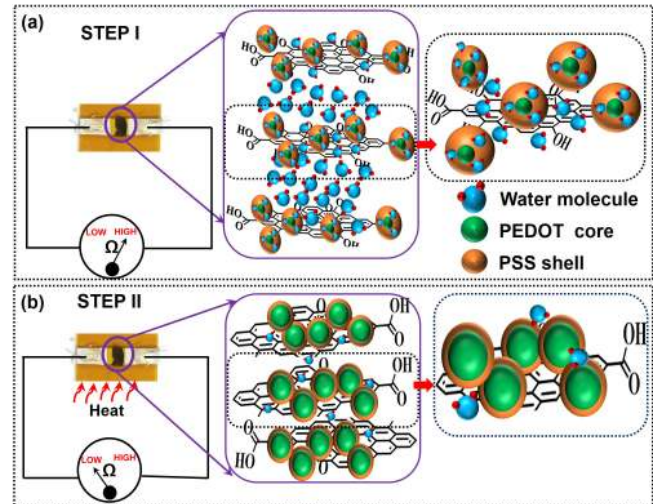

Fig. 3. Schematic illustration for microstructural changes in the sensitive layer leading to change in resistance at (a) RT (b) 100 °C.

flexible devices was insulated with Kapton tape (as discussed in Section II).

Afterwards, the temperature of the hot plate was gradually increased to 100 °C from RT (termed as heating). Once the temperature of the hot plate approached 100 °C, the printed GO/PEDOT:PSS demonstrates ∼80 % change in resistance. Based on the change in the electrical resistance of the sensor with temperature, Fig. 2(b) shows the response ($\Delta R/R_0 = (R - R_0)/R_0$, where ΔR is the change in resistance) of the sensor with variation in temperature from RT to 100 °C. It can be clearly seen from Fig. 2(b) that the printed GO/PEDOT:PSS based temperature sensor demonstrates around 80% change in resistance for a temperature change of ∼75 °C and sensitivity of more than 1.09% per °C. The calculated change in the resistance over temperature was found to be linear with a determination coefficient, r^2 value of 0.988, demonstrating the linearity of the sensor towards change in temperature.

For any temperature sensor, it is important to study the response and recovery times. As can be clearly seen from the first part of Fig. 2(a), the printed GO/PEDOT:PSS based temperature sensor shows a response time of 18 s. Additionally to study the recovery time, in the present investigations the printed GO/PEDOT:PSS based temperature sensor was carefully removed from the hot plate and allowed to cooldown while the resistance was being measured. While cooling the temperature at the surface of the sensitive layer was monitored continuously with a high precision IR thermometer (FLUKE 62 MAX). As seen from Fig. 2(a), the sensor takes around 32 s to completely recover (from 100 °C to RT).

As seen from Fig. 2 (a), the resistance of the samples was found to decrease with an increase in temperature, demonstrating a negative temperature coefficient (NTC) of resistance. Similar NTC characteristics for PEDOT:PSS based polymer composite is reported in the past [37], [38]. The two-step schematic illustration and explanation of various processes during the electrical characterization of the sensor for the NTC behaviour is shown in Fig. 3.

The PEDOT:PSS, generally has a core-shell grain-like structure, where the conductive PEDOT forms the core part and insulating PSS is the shell. GO is an insulator decorated with highly sensitive functional groups. Step I, at RT (Fig. 3 (a)), shows the hygroscopic nature of the PEDOT:PSS and GO makes them highly sensitive to water molecules [37], [38], [44]. Due to interlayer swelling of PEDOT:PSS the hydrogen bonds between the PSS weaken in the presence of water molecules [37], [38], [44], [49]. This leads to the increased distance between the conductive PEDOT and insulting PSS [37], [38], [44], [49]. The similar interlayer swelling is reported for GO in presence of water molecules, which is attributed to the generation of protons as a result of the reaction between water molecules and functional groups in GO [45], [50]. As a result of the combined effect of interlayer swelling, the movement of charge carriers in the GO/PEDOT:PSS composite is restricted which therefore leads to high electrical resistance. Increasing the temperature from RT to 100 °C (step II, Fig. 3(b)) weakens the hydrogen bonds between the water molecule and the PSS chain and this, in turn, reduces the interlayer swelling and in hydrogen bond attractions between PSS (either inter/intramolecular) [49]. Thus, the conductive core and insulting shell grains are interconnected. The thermal activation of GO conductivity, well-reported in past, is attributed to the loss (reduction) of functional group on heating and physio-chemical changes, leaving behind mobile ions, and resulting in semi/conducting nature, depending on the degree of reduction [22], [45], [50], [51]. The GO/PEDOT:PSS composite thus exhibits p-type semiconductor properties forming an acceptor impurity level near the valence band [38]. With the increase in temperature, the thermal energy increases and the electrons excited in the valence band are transferred to the conduction band. The hole left behind in the valence band results in an increased conductivity [38]. The higher sensitivity in the present investigation is most likely due to the electron hopping mechanism between adjacent polyaromatic molecules, similar to organic semiconductors [50].

In addition to this, for real-world and conformable applications, it is necessary to investigate the performance of the sensors under various static and dynamic bending conditions. Fig. 4 shows the response of printed GO/PEDOT;PSS based temperature sensors under various static bending (tensile and compressive) conditions over time and change in temperature (from RT to 100 °C). In the present investigations, a bending radius (r) of 10 mm, 20 mm and 30 mm was used for both (static tensile and compressive) bending conditions. At RT, no significant variation in the response of devices (under flat, tensile and compressive) was observed. However, when the temperature was gradually increased to 100 °C, less than ±5% variation was observed in the response time of the sensors when they were subjected to static bending conditions as compared with the flat sample. The change in the sensitivity of the sensors was negligible, as can be clearly seen from Fig. 4.

Apart from static bending conditions, the printed sensors were subjected to dynamic bending conditions (for up to
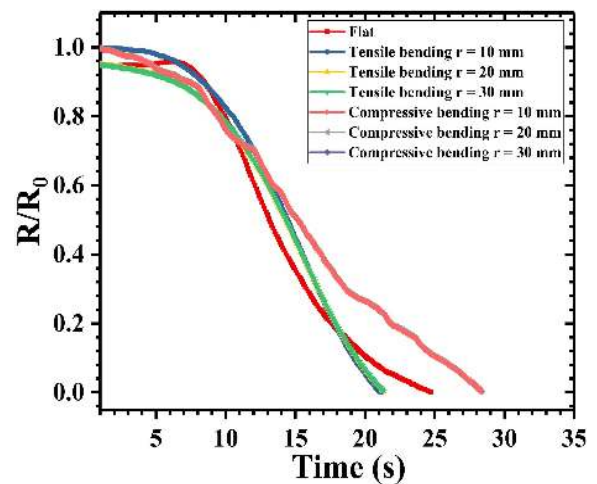

Fig. 4. Normalized change in the resistance of the sensors under different static bending (tensile and compressive) conditions over time with varying temperature (from RT to 100 °C).
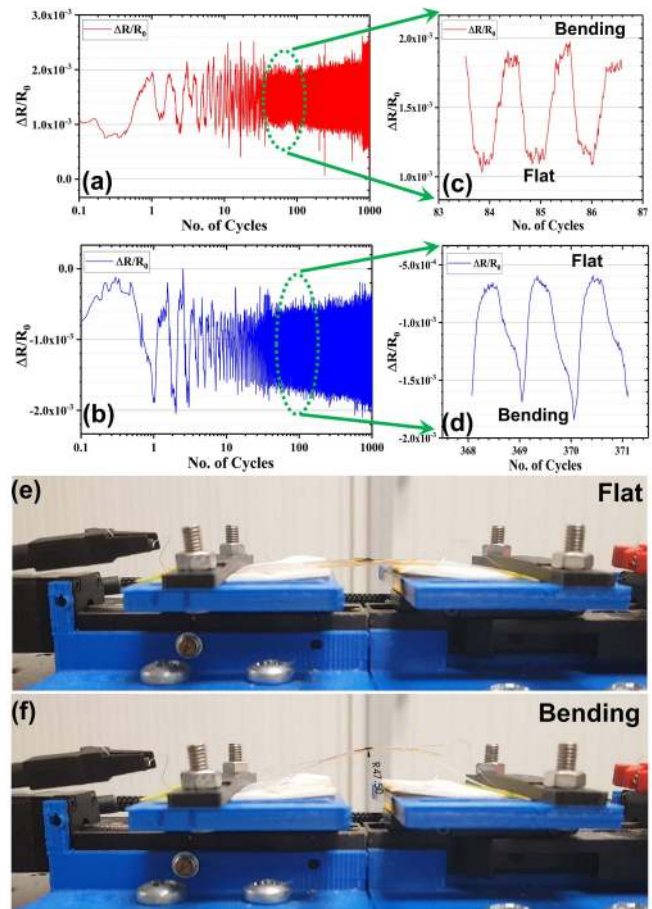
Fig. 5. Normalized resistance of the printed GO/PEDOT:PSS temperature sensor under dynamic (a) tensile (b) compressive bending cycles at RT. Zoomed in region showing three dynamic bending cycles for (c) tensile (d) compressive. Photograph of the sensor under (e) flat and (f) bending cycles.

1000 cycles) at RT to investigate the variation in the response of the senor. Fig. 5 summarizes the performance of the device for tensile and compressive bending conditions for over 1000 cycles. Both experiments were conducted with each bending cycle taking place every 5 seconds. For

Fig. 6. (a) CAD model of the 3D printed hand with the printed temperature sensor mounted on the thumb of a robotic hand, (b) Temperature sensor on distal phalanx of the thumb and in contact with a hot object and the response of the sensor, (c) Implemented feedback system with the hot object after threshold was reached. (d) the circuit diagram associated with the demonstration.
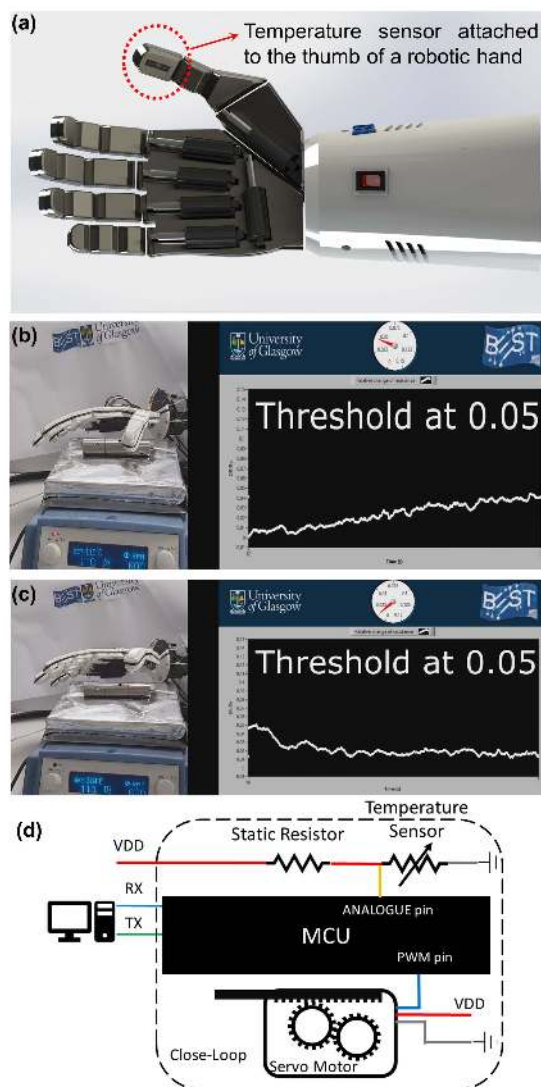

Fig. 7. Comparison of the printed temperature sensor with commercially available thermistor (100 kΩ). The marked regions show the response and recovery times for both the sensors.

both measurements, the samples were bent at a radius of $\sim$ 47.5 mm. Fig. 5(a) and 5(b) show the relative change of resistance during entire duration of experiments under tensile and compressive bending respectively. Fig. 5(c) and 5(d) shows three cycles at an arbitrary point of the experiments to demonstrate the repeatability of each cycle. Fig. 5(e) and 5(f) show the photograph of the sample under flat and bending conditions during the characterization procedure. The presented temperature sensor shows stable performance under bending conditions. From the dynamic bending, we observed an average change of 1% under bending condition. This small change can be considered negligible in comparison with the relative change of resistance with respect to temperature and can correspond to a difference in temperature of ($\sim$2 °C).

To demonstrate the application of the presented temperature sensor, the device was mounted on the distal phalanx of the thumb of a 3D printed robotic hand (Fig. 6 (a)) and the same was tested with heating arrangement (Fig. 6(b) and
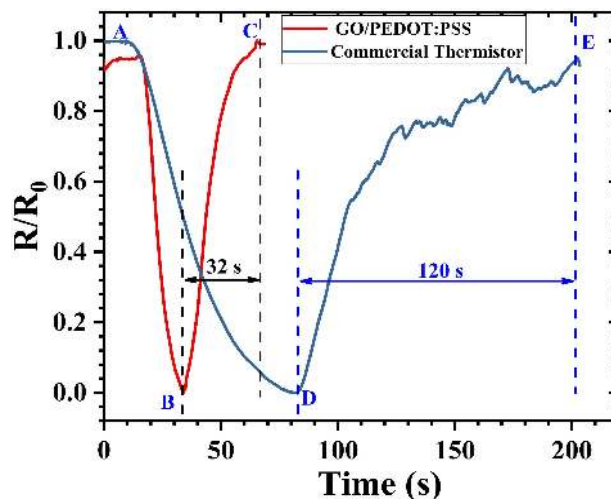
6(c)) [12], [52]. The readout circuit (Fig. 6(d)) comprises a voltage divider circuit. The voltage output of the circuit was captured by a microcontroller unit (MCU) as an analogue input. The data from MCU was sent to a PC and displayed using a LabVIEW program. A hot air gun was used to blow hot air on the thumb to measure the relative change in resistance of the sensor and evaluate its viability as a component of e-skin (Support Video 1). The temperature sensor was then tested with a feedback mechanism for preventing contact with hot objects as can be seen from Figure 6 (b) and Support Video 2. The finger is actuated via a linear servo motor, placed in the palm region and controlled using the same MCU. The system was configured to measure the voltage output of the sensor while a command was sent to the MCU to actuate the finger in contact with the object. After about 5 seconds of contact with the object, the output of voltage divider circuit reached the threshold 0.05 as indicated in Fig. 6(b) and 6(c), set in the system as safe temperature and the servo motor was immediately actuated to move the finger away from the object (Fig. 6 (c)). The reason for choosing the threshold $\Delta R/R_0 = 0.05$, is due to the fact that the sensing layer is not in contact with the hot object and heat transfer was done via proximity. The robotic hand was made using PLA material which can deform at temperatures above 70 °C.

Finally, the performance of printed temperature sensor was compared with a commercial thermistor (RS PRO Thermistor DO-35 100kΩ). The normalized resistance for the printed temperature sensor and the commercially available thermistor is as shown in Fig. 7. For comparison, the printed temperature sensor and the thermistor were placed on the hotplate at RT. The corresponding normalized resistance for the devices at RT is marked as "A" in Fig. 7. Gradually the temperature of the hot plate was increased to 100 °C at a rate of $\sim$3-4°C/s. As discussed previously, the printed temperature is highly sensitive to the temperature changes and demonstrates $\sim$ 80% change in resistance at 100 °C with a response time of 18 s (marked as B, in Fig. 7). In comparison, the commercial sensor showed $\sim$ 90% change in resistance at 100 °C but

TABLE I
SUMMARY AND COMPARISON FOR PRINTED FLEXIBLE
TEMPERATURE SENSOR

Sensitive Material	Temp. Range (°C)	Sensitivity (°C^1)	Response Time	Recovery Time	Ref.
Reduced GO	30 − 100	0.6	1.2 s for ΔT of 20 °C	∼ 7 s for ΔT of 20 °C	[8]
PEDOT:PSS	−50 − 80	0.48	–	–	[38]
CNT	20 − 75	0.24	–	–	[39]
CNT/PEDOT: PSS	21 − 80	0.25	1-2 s for ΔT of ∼2 °C	2-3 s for ΔT of ∼2 °C	[40]
Silver	20 − 60	0.2	–	–	[43]
P(VDF-TrFE)	25 − 75	0.5	–	–	[16]
P(VDF-TrFE)-BT	25 − 50	0.94	–	–	[21]
GO/PEDOT:PSS	RT − 100	1.09	18 s for ΔT of 75 °C	32 s for ΔT of 75 °C	This Work

the response time is about 65 s (marked as D, in Fig. 7). To evaluate the recovery time of the sensors, both the devices were removed from the hotplate (at 100 °C) and kept at room temperature to cool down to RT. The recovery path for the printed GO/PEDOT:PSS and commercial sensors are marked with B to C and D to E, respectively in Fig. 7. The GO/PEDOT:PSS sensor recovered completely after 32 s while the commercial sensor took ∼ 120 s to recover completely. Therefore, the printed GO/PEDOT:PSS based temperature sensor showed faster response as compared with the commercial thermistor. A further comparison of the performance of the presented printed flexible temperature sensor with other works reported in literature is given in Table I.

IV. CONCLUSIONS

To summarize, the printed flexible temperature sensor using silver paste and GO/PEDOT:PSS as conductive electrodes and sensitive layer, respectively is presented in this paper. The printed flexible temperature sensor demonstrated a negative temperature coefficient of resistance with ∼80% change in resistance and sensitivity of 1.09 % per °C with temperature varying from RT to 100°C. The advantages of the present approach include facile, cost-effective, scalable fabrication and compatibility with large area flexible substrates for eSkin applications. The printed sensor demonstrated stable and repeatable device performances when subjected to different static and dynamic bending conditions. The sensor was also integrated on a robotic hand and used to differentiate a hot object. As compared with the commercial thermistor, the printed flexible sensor showed about 4 times fast response and recovery times. As for the future, we aim to integrate the printed flexible temperature sensor with pressure/strain, humidity sensors along with the associated electronics to also extend the eSkin application to healthcare domain.

REFERENCES

[1] R. Dahiya, "E-skin: From humanoids to humans," *Proc. IEEE*, vol. 107, no. 2, pp. 247–252, Feb. 2019.
[2] D. H. Kim and D. C. Kim, "Stretchable electronics on another level," *Nature Electron.*, vol. 1, no. 8, pp. 440–441, 2018.
[3] R. Dahiya, D. Akinwande, and J. S. Chang, "Flexible electronic skin: From humanoids to humans," *Proc. IEEE*, vol. 107, no. 10, pp. 2011–2015, Oct. 2019.
[4] S. Khan, L. Lorenzelli, and R. S. Dahiya, "Technologies for printing sensors and electronics over large flexible substrates: A review," *IEEE Sensors J.*, vol. 15, no. 6, pp. 3164–3185, Oct. 2015.
[5] S. Xu, A. Jayaraman, and J. A. Rogers, "Skin sensors are the future of health care," *Nature*, vol. 571, pp. 319–321, 2019, doi: 10.1038/d41586-019-02143-0.
[6] T. Yokota *et al.*, "Ultraflexible, large-area, physiological temperature sensors for multipoint measurements," *Proc. Nat. Acad. Sci. USA*, vol. 112, no. 47, pp. 14533–14538, 2015.
[7] J. I. P. Quesada, F. P. Carpes, R. R. Bini, R. S. Palmer, P. Pérez-Soriano, and R. M. C. O. de Anda, "Relationship between skin temperature and muscle activation during incremental cycle exercise," *J. Therm. Biol.*, vol. 48, no. 10, pp. 28–35, 2015.
[8] G. Liu *et al.*, "A flexible temperature sensor based on reduced graphene oxide for robot skin used in Internet of Things," *Sensors*, vol. 18, no. 5, p. 1400, 2018.
[9] P. Sehrawat, S. Islam, and P. Mishra, "Reduced graphene oxide based temperature sensor: Extraordinary performance governed by lattice dynamics assisted carrier transport," *Sens. Actuators B, Chem.*, vol. 258, pp. 424–435, Apr. 2018.
[10] P. Webb, "Temperatures of skin, subcutaneous tissue, muscle and core in resting men in cold, comfortable and hot conditions," *Eur. J. Appl. Physiol. Occupational Physiol.*, vol. 64, no. 5, pp. 471–476, 1992.
[11] R. Dahiya, W. T. Navaraj, S. Khan, and E. O. Polat, "Developing electronic skin with the sense of touch," *Inf. Display*, vol. 31, no. 4, pp. 6–10, 2015.
[12] M. Ntagios, H. Nassar, A. Pullanchiyodan, W. T. Navaraj, and R. Dahiya, "Robotic hands with intrinsic tactile sensing via 3D printed soft pressure sensors," *Adv. Intell. Syst.*, pp. 1900080-1–1900080-9, 2019, doi: 10.1002/aisy.201900080.
[13] J. C. Yeo and C. T. Lim, "Emerging flexible and wearable physical sensing platforms for healthcare and biomedical applications," *Microsyst. Nanoeng.*, vol. 2, no. 1, p. 16043, 2016.
[14] M. Soni and R. Dahiya, "Soft eSkin: Distributed touch sensing with harmonized energy and computing," *Philos. Trans. Roy. Soc. A*, vol. 378, no. 2164, Feb. 2020, Art. no. 20190156.
[15] C.-Y. Lee, S.-J. Lee, M.-S. Tang, and P.-C. Chen, "*In situ* monitoring of temperature inside lithium-ion batteries by flexible micro temperature sensors," *Sensors*, vol. 11, no. 10, pp. 9942–9950, Oct. 2011.
[16] P. Tao *et al.*, "Bioinspired engineering of thermal materials," *Adv. Mater.*, vol. 27, no. 3, pp. 428–463, 2015.
[17] S. Hannah, A. Davidson, I. Glesk, D. Uttamchandani, R. Dahiya, and H. Gleskova, "Multifunctional sensor based on organic field-effect transistor and ferroelectric poly (vinylidene fluoride trifluoroethylene)," *Organic Electron.*, vol. 56, pp. 170–177, May 2018.
[18] R. S. Dahiya *et al.*, "Towards tactile sensing system on chip for robotic applications," *IEEE Sensors J.*, vol. 11, no. 12, pp. 3216–3226, Dec. 2011.
[19] S. Hannah, A. Davidson, I. Glesk, D. Uttamchandani, R. Dahiya, and H. Gleskova, "Multifunctional sensor based on organic field-effect transistor and ferroelectric poly(vinylidene fluoride trifluoroethylene)," *Organic Electron.*, vol. 56, pp. 170–177, May 2018.
[20] K. Takei, W. Honda, S. Harada, T. Arie, and S. Akita, "Toward flexible and wearable human-interactive health-monitoring devices," *Adv. Healthcare Mater.*, vol. 4, no. 4, pp. 487–500, Mar. 2015.
[21] S. Gupta, D. Shakthivel, L. Lorenzelli, and R. Dahiya, "Temperature compensated tactile sensing using MOSFET with p(VDF-TrFE)/BaTiO$_3$ capacitor as extended gate," *IEEE Sensors J.*, vol. 19, no. 2, pp. 435–442, Jan. 2019.
[22] M. Soni, P. Kumar, J. Pandey, S. K. Sharma, and A. Soni, "Scalable and site specific functionalization of reduced graphene oxide for circuit elements and flexible electronics," *Carbon*, vol. 128, pp. 172–178, Mar. 2018.
[23] X. Wang, L. Dong, H. Zhang, R. Yu, C. Pan, and Z. L. Wang, "Recent progress in electronic skin," *Adv. Sci.*, vol. 2, no. 10, Oct. 2015, Art. no. 1500169.
[24] A. Chortos, J. Liu, and Z. Bao, "Pursuing prosthetic electronic skin," *Nature Mater.*, vol. 15, no. 9, pp. 937–950, Sep. 2016.
[25] C. G. Núñez, L. Manjakkal, and R. Dahiya, "Energy autonomous electronic skin," *NPJ Flexible Electron.*, vol. 3, Jan. 2019, Art. no. 1, doi: 10.1038/s41528-018-0045-x.
[26] M. Amjadi, K.-U. Kyung, I. Park, and M. Sitti, "Stretchable, skin-mountable, and wearable strain sensors and their potential applications: A review," *Adv. Funct. Mater.*, vol. 26, no. 11, pp. 1678–1698, Mar. 2016.

[27] L. Manjakkal, W. T. Navaraj, C. G. Núñez, and R. Dahiya, "Graphene–graphite polyurethane composite based high-energy density flexible supercapacitors," *Adv. Sci.*, vol. 6, no. 7, Apr. 2019, Art. no. 1802251.

[28] M. A. Kafi, A. Paul, A. Vilouras, E. S. Hosseini, and R. S. Dahiya, "Chitosan–graphene oxide based ultra-thin and flexible sensor for diabetic wound monitoring," *IEEE Sensors J.*, to be published, doi: 10.1109/jsen.2019.2928807.

[29] M. A. Kafi, A. Paul, A. Vilouras, and R. Dahiya, "Mesoporous chitosan based conformable and resorbable biostrip for dopamine detection," *Biosensors Bioelectron.*, vol. 147, Jan. 2020, Art. no. 111781.

[30] S. Tong, J. Sun, and J. Yang, "Printed thin-film transistors: Research from China," *ACS Appl. Mater. Inter.*, vol. 10, no. 31, pp. 25902–25924, Aug. 2018.

[31] R. Dahiya *et al.*, "Large-area soft e-skin: The challenges beyond sensor designs," *Proc. IEEE*, vol. 107, no. 10, pp. 2016–2033, Oct. 2019.

[32] M. Soni, M. Bhattacharjee, L. Manjakkal, and R. Dahiya, "Printed temperature sensor based on graphene oxide/PEDOT: PSS," in *Proc. IEEE Int. Conf. Flexible Printable Sensors Syst. (FLEPS)*, Jul. 2019, pp. 1–3.

[33] M. Bhattacharjee, M. Soni, and R. Dahiya, "Microchannel based flexible dynamic strain sensor," in *Proc. IEEE Int. Conf. Flexible Printable Sensors Syst. (FLEPS)*, Jul. 2019, pp. 1–3.

[34] S. Khan, S. Tinku, L. Lorenzelli, and R. S. Dahiya, "Flexible tactile sensors using screen-printed P (VDF-TrFE) and MWCNT/PDMS composites," *IEEE Sensors J.*, vol. 15, no. 6, pp. 3146–3155, Jun. 2015.

[35] S. Khan, W. Dang, L. Lorenzelli, and R. Dahiya, "Flexible pressure sensors based on screen-printed P(VDF-TrFE) and P(VDF-TrFE)/MWCNTs," *IEEE Trans. Semicond. Manufact.*, vol. 28, no. 4, pp. 486–493, Nov. 2015.

[36] M. A. C. Angeli, F. Nikbakhtnasrabadi, P. Vena, and R. Dahiya, "Geometry dependent application of stretchable printed antenna," in *Proc. IEEE Int. Conf. Flexible Printable Sensors Syst. (FLEPS)*, Jul. 2019, pp. 1–3.

[37] T. Vuorinen, J. Niittynen, T. Kankkunen, T. M. Kraft, and M. Mantysalo, "Inkjet-printed graphene/PEDOT:PSS temperature sensors on a skin-conformable polyurethane substrate," *Sci. Rep.*, vol. 6, p. 35289, Oct. 2016.

[38] J.-W. Lee, D.-C. Han, H.-J. Shin, S.-H. Yeom, B.-K. Ju, and W. Lee, "PEDOT:PSS-based temperature-detection thread for wearable devices," *Sensors*, vol. 18, no. 9, p. 2996, Sep. 2018.

[39] K. S. Karimov, M. T. S. Chani, and F. A. Khalid, "Carbon nanotubes film based temperature sensors," *Phys. E, Low-Dimensional Syst. Nanostruct.*, vol. 43, no. 9, pp. 1701–1703, Jul. 2011.

[40] S. Harada, K. Kanao, Y. Yamamoto, T. Arie, S. Akita, and K. Takei, "Fully printed flexible fingerprint-like three-axis tactile and slip force and temperature sensors for artificial skin," *ACS Nano*, vol. 8, no. 12, pp. 12851–12857, Dec. 2014.

[41] G. Liu *et al.*, "A flexible temperature sensor based on reduced graphene oxide for robot skin used in Internet of Things," *Sensors*, vol. 18, no. 5, p. 1400, May 2018.

[42] M. Dankoco, G. Tesfay, E. Benevent, and M. Bendahan, "Temperature sensor realized by inkjet printing process on flexible substrate," *Mater. Sci. Eng., B*, vol. 205, pp. 1–5, Mar. 2016.

[43] Y. Chen, B. Lu, Y. Chen, and X. Feng, "Breathable and stretchable temperature sensors inspired by skin," *Sci. Rep.*, vol. 5, p. 11505, Jun. 2015.

[44] J. Zhou *et al.*, "The temperature-dependent microstructure of PEDOT/PSS films: Insights from morphological, mechanical and electrical analyses," *J. Mater. Chem. C*, vol. 2, no. 46, pp. 9903–9910, Sep. 2014.

[45] M. Soni, T. Arora, R. Khosla, P. Kumar, A. Soni, and S. K. Sharma, "Integration of highly sensitive oxygenated graphene with aluminum micro-interdigitated electrode array based molecular sensor for detection of aqueous fluoride anions," *IEEE Sensors J.*, vol. 16, no. 6, pp. 1524–1531, Mar. 2016.

[46] M. Soni, T. Arora, P. Kumar, A. Soni, and S. K. Sharma, "GO/μ-IDEs/p-Si based real time sensors for F-detection in natural drinking water," in *Proc. IEEE Int. Symp. Nanoelectron. Inf. Syst.*, Dec. 2015, pp. 272–276.

[47] W. Dang, L. Manjakkal, W. T. Navaraj, L. Lorenzelli, V. Vinciguerra, and R. Dahiya, "Stretchable wireless system for sweat pH monitoring," *Biosensors Bioelectron.*, vol. 107, pp. 192–202, Jun. 2018.

[48] W. Yan, J. Li, G. Zhang, L. Wang, and D. Ho, "A synergistic self-assembled 3D PEDOT:PSS/graphene composite sponge for stretchable microsupercapacitors," *J. Mater. Chem. A*, vol. 8, no. 2, pp. 554–564, Oct. 2019.

[49] A. Benchirouf *et al.*, "Electrical properties of multi-walled carbon nanotubes/PEDOT:PSS nanocomposites thin films under temperature and humidity effects," *Sens. Actuators B, Chem.*, vol. 224, pp. 344–350, Mar. 2016.

[50] S. Borini *et al.*, "Ultrafast graphene oxide humidity sensors," *ACS Nano*, vol. 7, no. 12, pp. 11166–11173, Dec. 2013.

[51] M. Soni, P. Kumar, R. Kumar, S. K. Sharma, and A. Soni, "Photocatalytic reduction of oxygenated graphene dispersions for supercapacitor applications," *J. Phys. D, Appl. Phys.*, vol. 50, no. 12, Mar. 2017, Art. no. 124003.

[52] W. Navaraj and R. Dahiya, "Fingerprint-enhanced capacitive-piezoelectric flexible sensing skin to discriminate static and dynamic tactile stimuli," *Adv. Intell. Syst.*, vol. 1, no. 7, Nov. 2019, Art. no. 1900051.

Mahesh Soni (Member, IEEE) received the master's degree in VLSI design from the National Institute of Technology Jaipur, India, in 2012, and the Ph.D. degree from the Indian Institute of Technology, Mandi, India, in 2018. After completing the Ph.D. degree, he joined the Bendable Electronics and Sensing Technologies (BEST) Research Group, University of Glasgow, U.K., as a Postdoctoral Fellow. His research interests include flexible electronic and memory devices, wearable sensors, and printed electronics.

Mitradip Bhattacharjee (Member, IEEE) received the B.Tech. degree in electronics and communication engineering from the National Institute of Technology, India, in 2013, and the Ph.D. degree from Indian Institute of Technology, Mandi, India, in 2018. He joined the Bendable Electronics and Sensing Technologies (BEST) Research Group, University of Glasgow, U.K., as a Postdoctoral Fellow, in 2019. His research interests include electronic sensors and systems, flexible/wearable and printed electronics, biomedical engineering, bioelectronics, and reconfigurable sensing antennas.

Markellos Ntagios received the B.Eng. (Hons.) degree in electronic engineering from the University of Bedfordshire, Luton, U.K., in 2017. He is currently pursuing the Ph.D. degree with the James Watt School of Engineering, Bendable Electronics and Sensing Technologies (BEST) Group, University of Glasgow, Glasgow, U.K.

Ravinder Dahiya (Fellow, IEEE) is currently Professor of electronics and nanoengineering with the University of Glasgow, U.K. He is the Leader of the Bendable Electronics and Sensing Technologies (BEST) Research Group. His group conducts fundamental and applied research in the multidisciplinary fields of flexible and printable electronics, tactile sensing, electronic skin, robotics, and wearable systems. He has authored over 300 research articles and 4 books. He holds 15 submitted/granted patents. He has led several international projects. He is currently the President-Elect and the Distinguished Lecturer of the IEEE Sensors Council. He is serving on the Editorial Board of *Scientific Reports*. He was the Technical Program Co-Chair of the IEEE Sensors 2017 and 2018. He has been the general chair of several conferences. He has received the prestigious EPSRC fellowship, the Marie Curie Fellowship, and the Japanese Monbusho Fellowship. Among several awards, he has received the 2016 Microelectronic Engineering Young Investigator Award and the 2016 Technical Achievement Award from the IEEE Sensors Council. He served on the Editorial Board of the IEEE SENSORS JOURNAL, from 2012 to 2020, and the IEEE TRANSACTIONS ON ROBOTICS, from 2012 to 2017.